

Julia Cloud Matrix Machine: Dynamic Matrix Language Acceleration on Multicore Clusters in the Cloud

Jay Hwan Lee
Yeonsoo Kim
Yonghyun Ryu
jlee758@yonsei.ac.kr
yeonsoo.kim@yonsei.ac.kr
Yonsei University
Seoul, South Korea

Wasuwee Sodsong
Hyunjun Jeon
Jinsik Park
Bernd Burgstaller
bburg@yonsei.ac.kr
Yonsei University
Seoul, South Korea

Bernhard Scholz
bernhard.scholz@sydney.edu.au
University of Sydney
Sydney, Australia

Abstract

In emerging scientific computing environments, matrix computations of increasing size and complexity are increasingly becoming prevalent. However, contemporary matrix language implementations are insufficient in their support for efficient utilization of cloud computing resources, particularly on the user side. We thus developed an extension of the Julia high-performance computation language such that matrix computations are automatically parallelized in the cloud, where users are separated from directly interacting with complex explicitly-parallel computations. We implement lazy evaluation semantics combined with directed graphs to optimize matrix operations on the fly while dynamic simulation finds the optimal tile size and schedule for a given cluster of cloud nodes. A time model prediction of the cluster's performance capacity is constructed to enable simulations. Automatic configuration of communication and worker processes on the cloud networks allow for the framework to automatically scale up for clusters of heterogeneous nodes. Our framework's experimental evaluation comprises eleven benchmarks on an fourteen node (564 vCPUs) cluster in the AWS public cloud, revealing speedups of up to a factor of 5.1, with an average 74.39 % of the upper bound for speedups.

Keywords: Matrix computations; Julia; HEFT; Distributed systems; Simulation; Parallel computing

1 Introduction

Matrix multiplication is a fundamental operation in scientific computing that has been extensively studied for parallel computing [3, 16, 48]. Utilizing a commodity cluster or the cloud for matrix computations is complex due to the required concurrency control mechanisms. In terms of performance, the bottleneck is often the network rather than the memory bandwidth of a single node [12]. To maximize the performance of large computations, splitting them into smaller

operations leverages parallelism, though at the cost of increased data communication. Striking a balance between the data communication bottleneck of the network and multicore parallelism is a key requirement to attain high performance in the cloud. Ideally, programmers are shielded from such considerations, if the underlying implementation of the sequential programming model can leverage the inherent parallelism for efficient execution in the cloud. This particularly applies to matrix languages like MATLAB, Octave, and Julia, which are designed for programmer productivity and abstraction from the underlying multicore substrate, rather than hand-optimization of hardware-dependent code. To automatically parallelize matrix computations, our approach uses lazy evaluation with hierarchical dependency analysis, online scheduling, and simulation to effectively run tasks in parallel and reduce the impact of the network on performance. We implement this in Julia, a dynamic language for high performance computing that is already equipped with a robust, explicitly-parallel programming model [8]. The contributions of this paper are as follows.

- The Julia cloud matrix machine (Julia CMM) that extends the Julia programming language with implicitly-parallel matrix routines for the cloud through an extension of the Julia matrix data type.
- An online simulation and run-time that employs a time model based on offline profiling and regression analysis to predict task execution times. We utilize this in conjunction with automated matrix parallelization and communicator configuration to both predict the most efficient schedule of task parallelization across a cluster of cloud nodes and to adjust the optimal distribution of communication and computation processes for each node.
- An extension of the HEFT scheduling algorithm that employs a node-level tile cache and a dynamic tiling optimization to reduce the network-incurred communication bottleneck.

Abbreviations: AWS, Amazon Web Service; HEFT, Heterogeneous Earliest Finish Time; CMM, Cloud Matrix Machine

- An extensive experimental evaluation on the AWS public cloud with homogeneous and heterogeneous clusters to show the validity of our approach.

2 Related Work

The computations in level 1 Basic Linear Algebra Subprograms (BLAS) involve vector-vector operations [26], whereas level 2 BLAS focuses on vector-processing machines [14]. Level 3 BLAS is designed to leverage caches in a multi-memory hierarchy [13]. To optimize cache utilization, matrices are divided into smaller matrices to achieve higher cache hit ratios [49, 50]. In Julia, OpenBLAS [39] is used as a multi-threaded level 3 BLAS implementation for linear algebra operations. Although research has been conducted on parallelizing BLAS operations for distributed systems [9, 40], the existing methods provide low-level BLAS operations, a static communication model, and fixed tile sizes. The proposed Julia CMM, on the other hand, offers a high-level programming abstraction, a dynamic communication model, and adaptable tile sizes. Julia’s standard library includes the RemoteChannel and SharedArray primitives for intra- and inter-node communication. However, programmers must manually parallelize their Julia code for cloud computing. Several studies report that the network bandwidth for intra-node communication is the main limiting factor of matrix operations and try to model and optimize the communication cost [11, 32]. In addition to intra-node communication bandwidth, our Julia CMM considers the inter-node communication, dependencies of operations, and the number of communication and computation processes in optimization.

Numerous studies have explored automated parallelization of matrix operations, including optimization compilers [5, 43] and generating optimal parallel algorithms for matrix-vector multiplication in neural networks [33]. Ongoing research focuses on optimizing matrix multiplication for Intel processors [20, 34], but this work does not involve implicit parallelism like that offered by Julia CMM. To address load imbalances, researchers have developed hybrid versions of breadth-first search (BFS) and depth-first search (DFS) algorithms for task-based parallelism [6], auto-tuning of sparse matrix-vector multiplication on multicore clusters with thread and process-based communication [28], tiling of sparse matrix-matrix multiplication on GPUs [35], automation of stream parallelism in C++ [30], and a modified selection prioritization HEFT algorithm for cloud environments [19]. These frameworks, however, do not implement implicit parallelization for general matrix operations and may be more suitable for expert programmers than for domain experts or novice users.

Alternative implementations of the HEFT algorithm aim to address load imbalance issues in cloud networks, especially those that reduce throughput by creating idle resources when parent and child tasks with different input instances

are processed in parallel [54]. On the other hand, E-HEFT reduces the number of communication tasks, and its scheduler distributes tasks across nodes, followed by running a simulation [42]. To reduce communication tasks, we already utilize node-level tile cache and have implemented a separate scheduler and simulation as described in the paper. Conversely, EHEFT-R employs remapping resource allocation rules to synthesize optimal machines for ranked tasks [53]. However, ranking is not an effective optimization in a network where all machines are equal.

Scientific workflow research involves structuring computations connected through dependencies [45] as a model for large-scale applications. Different tasks are scheduled to parallel resources, with task scheduling optimization being an NP-complete problem [47]. Heuristic scheduling algorithms are introduced for cloud computing service providers to minimize load imbalance between users of their large-scale cloud computing platforms [24, 38, 52]. While load balancing heuristics are applicable to Julia CMM in improving the parallelizable performance, such heuristic algorithms aim to optimize the load balancing between all users of the cloud, while Julia CMM’s goal is to achieve the shortest makespan of matrix operations as a single user. In a cloud environment, optimizing resource usage costs serves as an additional optimization point. Researchers proposed multi-objective scheduling algorithms [15, 31] to meet multiple optimization objectives in a cloud environment, noting that doing so inevitably results in trade-offs.

3 Julia CMM Framework

In Step 1 of Figure 1 step ①, Julia CMM demonstrates minimal invasiveness for the user, as it only requires the casting of matrices to the provided ClusteredMatrix data type (lines 2-3) to parallelize sequential matrix code, such as the depicted Markov chain computation, without altering the actual computations (lines 5-9). The user writes code in a Jupyter notebook [2], which serves as the frontend on their desktop or laptop. Julia CMM connects to the user’s cloud instances via an MPI-like configuration file, listing the IP addresses of the cluster nodes and designating one node as the master.

Despite being initiated by users on their local machines, the actual computations of Julia CMM take place in the cloud. The framework adopts lazy evaluation, which means that during runtime, it substitutes the execution of matrix operations with the construction of an expression tree. The actual computation of operations is deferred until the result is needed. For example, in Figure 1 step ①, the for loop iterates three times, followed by the multiplication $u * M$, leading to the creation of the expression tree illustrated in Figure 1 step ②. The display statement in line 11 triggers the actual computation of the tree, as it necessitates the output of the result to the user.

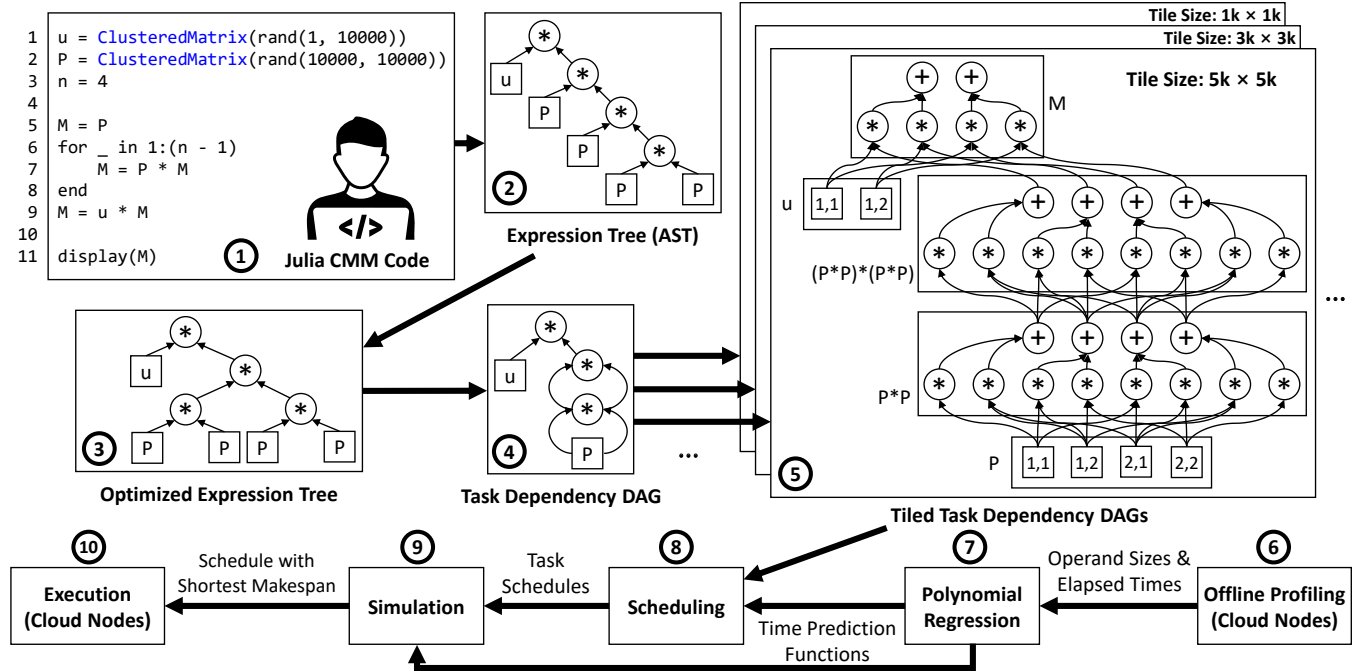


Figure 1. Overview of Julia CMM, depicting the on-the-fly lowering of the Markov chain benchmark source code ① to an expression tree ② that is then optimized by employing exponentiation by squaring ③. Common subexpression elimination creates a task dependency DAG ④ which is lowered further into tiled task dependency DAGs ⑤ for a series of standard tile sizes (here $1k \times 1k$, $3k \times 3k$, and $5k \times 5k$). Online scheduling ⑧ and simulation ⑨ of each of the tiled task dependency DAGs is used to determine the schedule with the smallest—predicted—makespan, which is then executed on the cluster of cloud nodes ⑩. The framework’s time model is based on offline profiling ⑥ and regression analysis ⑦.

Lazy evaluation provides the advantage of aggregating operations before their execution, thereby broadening the *scope* of optimization and parallelization beyond individual operations, such as those in BLAS, to contiguous regions of operations in the execution trace. In the context of our example, this wider optimization scope allows the framework to identify the matrix exponentiation operation embedded in the expression tree (i.e., $P * P * P * P$) and rewrite it using exponentiation-by-squaring, as shown in step ③ and discussed further in Section 3.1. The elimination of the common subexpression $P * P$ reduces the number of matrix multiplications in the resulting task dependency DAG, as illustrated in step ④.

The use of lazy evaluation in Julia CMM widens its parallelization scope, allowing it to balance the amount of parallelism with the communication overhead involved in tiling matrix operands into sub-operands (herein called tiles). Tiling is necessary to reduce the granularity of work and utilize the parallel execution units of a cluster, but it increases communication overhead. Figure 1 step ⑤ shows how Julia CMM transforms a task dependency DAG into a series of tiled dependency DAGs, each encoding the *entire* task dependency DAG for a specific tile size. By creating tiled DAGs for a range of standard tile sizes, Julia CMM conducts an online

simulation to predict the makespan of each tiled DAG and selects the one with the shortest makespan for execution on the given cluster. This approach enables the framework to effectively balance parallelism and communication overhead in the trade-off.

To optimize the execution time of tiled DAGs, we use an online simulation with a time model that is obtained from offline profiling. This allows the re-use of profile data for known instance types and locations. We employ a modified version of the HEFT algorithm to generate task schedules that optimize the earliest finish times of tiled DAGs. After the master node determines the schedule with the shortest makespan, it uses worker processes on both the master and worker nodes to execute the schedule. The workers send their computed results back to the master node, from where the results are output to the user on their client machine.

3.1 Tree-rewriting, Tiling, Scheduling & Simulation

In Figure 1, we illustrate the process from `ClusteredMatrix` in Julia CMM to tiled dependency graphs on the master node using a Markov chain computation. The figure depicts references P and u , which point to `ClusteredMatrix` objects generated from random matrices based on the given input dimensions. As shown in step ② of Figure 1, matrix P is

```

1 function tile(P::ClusteredMatrix, tile_size::Tuple)
2     mP, nP = size(P)
3     mTile, nTile = tile_size
4     mTiledP, nTiledP = cld(mP, mTile), cld(nP, nTile)
5     tiledP = Matrix{ClusteredMatrix}(mTiledP, nTiledP)
6
7     for j=1:nTiledP
8         colStart = nTile * (j-1)+1
9         colEnd = min(nTile * j, nP)
10        colIdx = colStart:colEnd
11        for i=1:mTiledP
12            rowStart = mTile * (i-1)+1
13            rowEnd = min(mTile * i, mP)
14            rowIdx = rowStart:rowEnd
15            tiledP[i,j] = view(P, rowIdx, colIdx)
16        end
17    end
18    return tiledP
19 end

```

Listing 1. Implementation of the tile function

multiplied by itself three times before its final multiplication with matrix u , represented in the expression tree.

The construction of an expression tree involves tracing the matrix operations performed at runtime by overloading the operators of the `ClusteredMatrix` data type. The input dependencies between the edges of the expression tree are used to build the task dependence graph. Julia CMM implements lazy evaluation, which defers the actual execution of matrix operations until a user-observable side-effect is reached or until the trace exceeds a predetermined threshold. Once this occurs, Julia CMM pattern-matches the expression tree to rewrite sub-trees for which a more efficient equivalent is known to exist. This approach eliminates common subexpressions [4] and transforms series of multiplications into the exponentiation-by-squaring method [22]. By contrast, standard Julia cannot perform this optimization unless the user manually replaces the for loop in Figure 1 with Julia’s exponentiation operator.

In addition to exponentiation by squaring, further matrix algebraic optimizations in our implementation include (1) computing Moore-Penrose pseudo-inverse of matrices, particularly for use with the optimization of calculating non-square matrix computations for benchmarks with least square operations or sparse matrices [17]; (2) hierarchical singular value decomposition (HVSD) for optimizing dense matrix computations through reducing dimensionality while increasing parallelizability [37]; (3) computing matrix power through diagonalization, only for applicable matrices that are capable of being diagonalized [25]; (4) for equations involving commutative matrix rings, employing an application of the fast commutative matrix algorithm in reducing the number of multiplication operations [41]. These algebraic optimizations are of high opportunity and profitability, as shown by our experimental evaluation in Section 4.

We note that as floating-point operations are not associative, there is the possibility of a loss of precision. As demonstrated in a study of Strassen’s algorithm (which involves matrix partitioning) on Julia, double precision, `Float64`,

is found to result in the most efficient precision particularly for larger matrix sizes, with a maximum absolute error of 10^{-14} for a matrix size of 1 k [36]. We already utilize `Float64` in Julia CMM to reduce the degree of error, but acknowledge it does not fully mitigate it.

The size of tiles used in partitioned matrix operations determines the granularity and level of parallelism. Smaller tiles increase parallelism but result in a larger number of suboperations and increased communication overhead. We conducted experiments on both AWS cloud and our commodity cluster, and observed that a tile size in the range of 10–50 % of the matrix size provides optimal results for most benchmarks. However, tile sizes exceeding 50 % do not provide enough parallelism. To determine the optimal tile size, we use time simulation with time models instead of actual execution times, and generally use a sequence of tile sizes (1 k, 3 k, and 5 k) for a matrix size of 10 k, with 5 k being the best choice for most benchmarks of that size.

In Figure 1, the tile size of 5 k was predicted to have the shortest makespan for the input matrix of size 10 k. Using this tile size, the automatic tiling framework created four partitioned tiles of dimensions $5\text{ k} \times 5\text{ k}$ from matrix P , and two tiles of dimensions $1 \times 5\text{ k}$ from matrix u . The dependency graph was updated to reflect the tiles, while maintaining the task dependencies.

To generate a tiled matrix, we use the algorithm shown in Listing 1, which takes a matrix and tile size as arguments. In lines 4–5, we make use of `cld`, which returns the smallest integer that is greater than or equal to the division of the input matrix’s dimension by the input tile size’s dimension, thereby resulting in the number of tiles to generate. A tiled matrix with tiles separated by tile dimensions (lines 8–15) is returned as a `ClusteredMatrix`, with tiles stored in a list following the input matrix’s ordering. The process can be repeated for generating further sub-tiles.

3.2 Dynamic Tiling Optimization

To avoid underutilizing CPU cores on worker nodes, it is crucial to promptly propagate data and compute tasks to worker nodes as soon as the master node begins executing the selected schedule. We refer to the time duration from the start of a schedule until every worker has received computation tasks as the *startup phase*. As shown in Figure 2a, the upper half depicts the schedule of the master node, while the bottom half represents one worker node. Time progresses from left to right. The green rectangles represent data send operations, and the two green bars at the top of the figure indicate that the two communication processes in the master node continuously send data across the network to the worker node labeled “Worker 1”. The red rectangles represent compute tasks, and the blue arrow in the bottom-left of the figure indicates that it takes almost 0.75 s into the schedule until all three worker processes of Worker 1 have

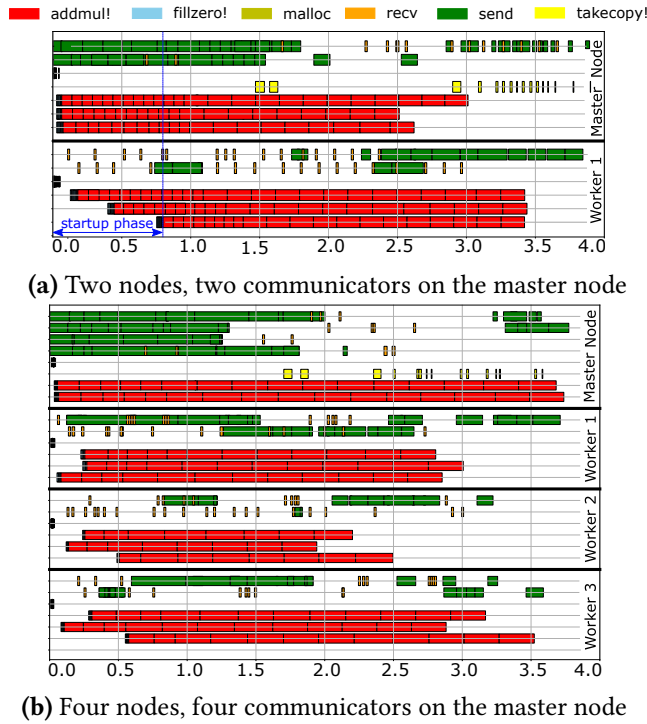


Figure 2. Markov chain benchmark task schedules for two cluster configurations of two and four nodes on AWS c5.9xlarge instances using matrix sizes of 10 k and tile sizes of 3 k. Time flows from left to right. Schedules are visualized on a 4 s timeline to facilitate comparisons. Data send tasks (green) and matrix computations (red) dominate the schedules. The length of receive tasks (orange) is shorter than the corresponding send tasks.

begun computations. (Note that there are several matrix zeroing tasks represented by blue rectangles at the beginning of the schedule, but they are of small duration and are not the constraining factor for the makespan; the limiting factor is the time until data has arrived from the master node.)

The limited bandwidth of network communication poses a challenge in the efficient distribution of matrix data to worker nodes during the startup phase. In particular, large matrix tile sizes can monopolize the network and cause delays in communication with other nodes, resulting in idle workers or those that do not receive data at all. To address this issue, we propose a dynamic tiling approach in the startup phase. Our method involves the dynamic adjustment of tile sizes, where larger tiles are split into smaller sub-tiles to enable more operands to be sent across the network in the same amount of time. This generates a heterogeneous collection of tiles, with smaller tiles being prioritized over larger ones to maintain dependencies. During scheduling, sub-tiles are prioritized to bring work to all workers within a shorter duration. After all nodes receive work, sub-tiles are combined back into tiles in-place, allowing the original tile sizes to be utilized in subsequent matrix operations. This

approach ensures that all workers are utilized efficiently during the startup phase, resulting in improved performance and reduced idle time.

Figure 2 shows that during the startup phase, the worker nodes experience a significant downtime as they wait to receive data from the master node. In the absence of dynamic tiling, this downtime is even more severe and may result in some worker nodes not receiving any tasks, particularly in larger networks. However, by using dynamic tiling, smaller tasks are staged at the beginning of the schedule, reducing communication costs *per task* and minimizing the downtime. As described in Section 4, the use of dynamic tiling leads to an overall speedup of $\geq 10\%$ for most benchmarks.

We further extend the tiling process by parallelization. After a matrix is partitioned into tiles, each tile is concurrently split into sub-tiles until the desired tile sizes are achieved – after which all sub-tiles are aggregated for use in the scheduling phase.

3.3 Offline Profiling & Time-Model Construction

Ensuring minimal total execution time in task allocation requires accurate prediction of each task’s execution time. In this study, we employed off-line profiling on a selection of typical matrix operations to construct the Julia CMM time model. Time measurements were based on CPU timestamp counters (TSCs). To overcome measurement errors across nodes where TSCs are typically unsynchronized, we employed a novel technique that ensures the measurement error remains below $500\ \mu\text{s}$ [51]. The off-line profiling step was performed only once for a given cluster configuration.

To construct the time model, we utilized multivariate polynomial regression analysis based on the ordinary least squares (OLS) method [23]. The amount of data used in this analysis is proportional to the matrix size and the number of floating point operations. Therefore, we made use of polynomial equations to predict the execution time. Table 1 outlines the classification for the interpolation equations used in constructing the time predictions, where the number of floating point operations is represented by a multivariate polynomial parameterized by the matrix size. The constants used in the equations were obtained through regression analysis, separately for each node and each node-to-node network link.

3.4 Memory Management and Node-level Tile Cache

When parallelizing a matrix operation, it is divided into smaller sub-operations that require certain operands, which may be needed by multiple succeeding operations (I.e., such an operand will have multiple successors in the dependency DAG, as illustrated in Figure 1). This leads to redundant inter-node communication, where data is repeatedly sent to the same node. To address this issue, we introduced a node-level tile cache using a SharedArray (from the Julia standard library) in the main memory of each node. The

Table 1. Interpolation based on the operand and operator sizes. The first two columns are the left and right operands, followed by the operators and the interpolation equation.

L Operand	R Operand	Operator	Interpolation Eqn.
$(n, 1)$	$(n, 1)$	$+, -, x$	$a_0 + a_1n$
$(nm, 1)$	$(n, 1)$	x	$a_0 + a_1n + a_2m + a_3mn$
(m, n)		\sin, \cos	$a_0 + a_1n + a_2m + a_3mn$
(m, n)	1	$+, -, x, /$	$a_0 + a_1n + a_2m + a_3mn$
(m, n)	(m, n)	$+, -, x$	$a_0 + a_1n + a_2m + a_3mn$
(m, n)	(n, k)	x	$a_0 + a_1n + a_2m + a_3k + \dots + a_7mnk$

SharedArray data type allows processes on the same node to share data, thus reducing the need for inter-node communication. The cache is controlled by the scheduler, with commands for placement and eviction of operands already part of the schedule, rather than guided by heuristics. The simulator accounts for the node-level tile caches in its predictions. Table 2 illustrates the performance improvements achieved by the node-level tile cache at various tile and network sizes.

3.5 HEFT Scheduler Extension

To improve scheduling efficiency, we enhance the heterogeneous earliest-finish-time (HEFT [46]) algorithm by incorporating the node-level tile cache awareness. The algorithm consists of two phases: task prioritization and assignment. During the prioritization phase, tasks are ranked recursively based on their average computation and communication costs across all nodes. In the assignment phase, tasks are assigned to processors such that the earliest finish time is selected. We employ the average internode communication costs and dynamically adjust the communication costs based on the presence of tiles in the node-level cache. In addition, we use the time predictions discussed in Section 3.3 to estimate the duration of each task. The scheduler accounts for communication time, which involves a send task from the sender and a receive task from the receiver, as shown in Figure 2. The algorithm gives priority to smaller tile sizes during task prioritization. The accuracy of the schedules generated is dependent on the accuracy of the cost predictions.

During the startup phase of the schedule, there is always a slight delay in which worker nodes must wait to receive data from the master. To minimize finish times, the scheduler prioritizes earliest finish time and initially favors worker processes on the master node, which has no communication requirements. However, since the capacity of the master node is limited, worker nodes are used to reduce finish times. The scheduler rejects scheduling on a node if the predicted combined communication and computation time is longer than waiting for a node where the tile is already present to become available. Because the master communicates with all workers, it has more dedicated communication processes to handle multiple communication tasks simultaneously, which

Table 2. Simulated execution times of the Markov benchmark with and without the node-level tile cache. Profiled data was obtained from AWS c5.9x large instances (nodes) at a matrix size of 10 k.

Name	w/ cache	2 Nodes				8 Nodes			
		1k	3k	5k	7k	1k	3k	5k	7k
Markov	Y (s)	4.92	3.61	2.97	12.69	3.77	2.92	1.57	10.23
	N (s)	5.38	3.94	3.23	12.92	5.25	3.89	3.12	11.01
Kmeans	Y (s)	8.85	6.80	6.10	11.17	5.74	3.34	2.37	7.43
	N (s)	9.25	7.17	6.78	12.26	6.21	3.99	2.51	8.54
Hill	Y (s)	6.36	3.85	3.30	11.80	3.78	2.81	1.56	9.92
	N (s)	7.35	4.25	3.79	12.13	4.01	3.05	1.92	10.72
Leontief	Y (s)	9.70	8.78	7.98	15.81	6.58	5.05	4.01	11.77
	N (s)	10.56	9.82	8.80	16.62	6.89	5.49	4.43	12.60
Synth	Y (s)	6.47	4.83	4.82	12.69	3.97	3.09	1.40	11.60
	N (s)	7.23	5.28	5.62	13.86	5.14	4.16	3.34	12.28
Reach.	Y (s)	8.69	8.33	7.24	16.08	5.94	4.94	4.19	13.21
	N (s)	9.11	8.85	7.42	16.41	6.38	5.55	4.56	14.07
Hits	Y (s)	9.24	6.99	6.98	16.69	5.83	4.27	2.92	10.28
	N (s)	10.05	7.68	7.49	17.08	6.33	5.09	3.34	11.07
BFS	Y (s)	27.31	22.22	18.55	24.92	14.88	9.38	6.70	16.90
	N (s)	29.44	25.53	20.43	26.18	16.93	11.39	8.06	17.95
MM	Y (s)	36.91	31.93	23.47	33.00	13.90	13.50	10.77	21.93
	N (s)	39.04	34.91	26.53	35.31	16.45	15.90	12.90	23.07
SPMV	Y (s)	43.05	37.09	27.14	39.81	25.64	19.83	14.78	26.81
	N (s)	48.24	41.74	34.47	43.02	30.58	26.30	28.42	31.72
Montage	Y (s)	65.30	53.14	41.89	73.28	29.69	24.21	16.63	63.58
	N (s)	81.63	71.50	60.06	85.80	48.33	47.85	49.65	77.81

reduces load imbalance caused by communication tasks waiting to be scheduled.

Figure 3a shows the speedup improvement obtained from allocating more communication processes to the master node in a heterogeneous cluster, improving the schedule execution time from 3.4 s to 2.2 s. With the heterogeneous cluster, Julia CMM makes use of an automatic communicator configuration (discussed further in Section 3.6) to automatically select the instance with the higher compute and network capacity as the master node.

For each node, the online simulator takes into account the duration of ongoing computation tasks, the number

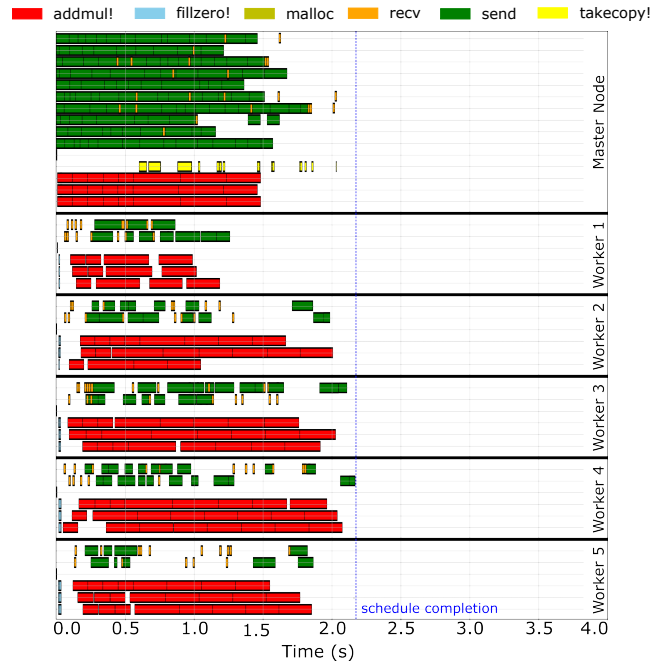
of available cores, the node’s communication bandwidth, and whether the upcoming task’s dependencies are already cached in the node (if not, further communication costs are incurred). If multiple candidate nodes are found where they have available cores and are ranked the same in bandwidth limit, the scheduler will tentatively tile the upcoming task and simulate the results. The scheduler then selects the node resulting in the earliest finish time, then moves on to the next task.

We note that the scheduler generates different schedules *in parallel*, evaluating different numbers of workers and communicators in the master node, based on the upper bandwidth limit and number of cores determined during the profiling stage (cf. Table 9 and Table 10). Once all schedules have been computed, the schedule that results in the smallest makespan is selected. This parallelization thereby minimizes the execution-time overhead of the simulation. Our experimental evaluation in Section 4 shows that the simulation overhead is below 0.2 s on average.

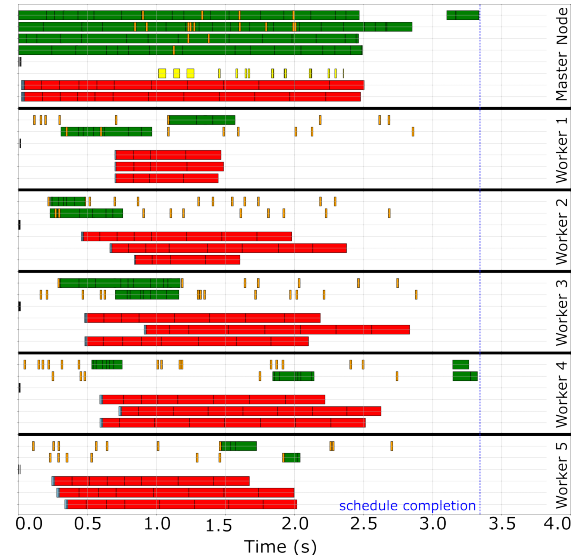
3.6 Automatic Communicator Configuration

In Julia CMM, each node in the network is assigned a set number of communication and worker processes. One worker process comprises of the number of threads configured for BLAS, while one communication process contains one thread. Thus, a node with two communication processes and three worker processes has a total of 14 threads operating. Our experiments make use of the Amazon EC2 service, where we utilize the instance type c5.9xlarge [1], each of which provides 36 vCPUs (18 physical cores) and a guaranteed 10 Gbps bandwidth in a shared network. Table 3 shows the GFLOPS numbers for our framework based on the number of threads configured for an AWS c5.9xlarge instance. We find that resource oversubscription in a given node occurs at 16 threads or more. One c5.9xlarge instance has 36 vCPUs and 18 physical cores. Thus, adding more worker threads than the number of physical cores in a node causes thread contention utilizing resources, outweighing any potential benefit from introducing more worker processes.

As discovered from our dynamic tiling approach, the number of communication processes on the master node limits the extent to which parallelism can take place in a shared network. Thus, in scaling the framework to larger scales, the necessity of utilizing a cluster of heterogeneous nodes increases. In such a setup, it is advantageous for the framework to allocate the most powerful node as the master, as more communication processes can be allocated to each of its physical cores. To facilitate this transition, we implement an automatic communicator detection and communication feature. During the profiling phase, for each node, Julia CMM automatically obtains the maximum number of available threads based on the number of cores retrieved by Julia’s `Sys.CPU_THREADS` command. A small benchmark is run in



(a) Six nodes, cluster of heterogeneous nodes



(b) Six nodes, cluster of homogeneous nodes

Figure 3. Markov chain benchmark task schedules for a cluster of heterogeneous nodes and a cluster of homogeneous nodes. The heterogeneous cluster contained one AWS c5.24xlarge instance that was automatically selected by the framework as the master node, and all other (worker) nodes were AWS c5.9xlarge instances. The benchmark uses a matrix size of 10 k and tile sizes of 3 k. Both schedules have six nodes in the network. Time flows from left to right. Schedules are visualized on a 4 s timeline to facilitate comparisons. Julia CMM’s capacity for running on a heterogeneous cluster allows the deployment of a master node with a higher capacity for computation and communication, thereby shortening the startup phase from 0.81 s to 0.22 s resulting in a 359 % speedup, and the overall makespan from 3.4 s to 2.2 s resulting in a 155 % speedup.

the network, where each node continuously sends and receives of empty communication requests. The number of communication processes for the master node is incrementally increased until either a saturated network bandwidth is detected (where further increases do not result in communication performance improvement), or until there are no available cores to allocate communication threads to (depending on the number of threads configured for BLAS, up to two worker threads are first allocated for the master node, and the remaining threads are checked for communication availability). If an excess number of cores are left over after network bandwidth saturation, they are allocated to new worker processes.

Furthermore, as part of the communication profiling, it monitors the inter-node network traffic flow and periodically records the maximum data bandwidth between pairs of nodes, the number of cores for each node, and the number of tasks before saturation is reached. Scheduling utilizes such profiled information to identify node-to-node links where a node’s maximum bandwidth or number of cores is lower than its peers and rank the nodes in order of decreasing strength, prioritizing the placement of bandwidth capacity over computational power. The task and tile distribution is accordingly adjusted where lower ranked nodes are assigned fewer tasks until either the bandwidth is saturated or the nodes are unable to process more work, and favoring higher ranked nodes where bandwidth is not as big of a bottleneck.

Some degree of configuration by the user is required in the allocation of BLAS threads and maximum number of worker processes for the master and worker nodes. However, the automatic configuration opens up Julia CMM to be pliable for clusters of heterogeneous nodes without necessitating deep manual intervention to match different node configurations.

4 Experimental Evaluation

Due to space constraints, for several aspects of our evaluation only a subset of the data sets from the paper’s accompanying technical report [27] is presented (and indicated as such).

To evaluate Julia CMM, we adopted benchmarks from a Cell Octave benchmark set [21], a set of highly parallelizable applications. We specifically took the Markov, K-Means, Hill, Leontief, Synth, Reachability, and Hits benchmarks and rewrote them in the Julia language. The Parboil Benchmark set [44] contains a set of throughput benchmarks for testing computer architecture in CUDA and OpenCL. We specifically adapted the BFS, MM, and SPMV benchmarks, which use matrix operations more predominantly than the others, and ported them to Julia. Pegasus [10] is a programming language for workflow applications such as CyberShake (earthquake testing) [18] and Sipht (searching untranslated RNAs) [29]. Pegasus utilizes DAGs in reproducing and analyzing scientific workflows, which share similarities with the schedules generated with our Julia framework. One application that

Table 3. GFLOPS performance of an AWS c5.9xlarge instance with Julia CMM, over 25 runs. We state the total number of threads, communicators per worker node, workers (and threads per worker), GFLOPS, and the coefficient of variation.

Total No. threads	Comm.	Workers (threads)	GFLOPS Avg.	CoV (%)
4	1	3(1)	2,257.8	3.6
8	2	3(2)	1,186.3	5.9
12	3	3(3)	822.3	5.3
14	2	3(4)	720.9	7.3
16	4	3(4)	628.6	4.1
32	4	7(4)	629.1	6.5
64	8	7(8)	628.6	6.8

uses Pegasus is the Montage Image Mosaic Engine [7], a tool for assembling astronomical input images into custom mosaics. We ported the Montage workflow written in Pegasus over to Julia that computes three separate color matrix channels to generate a small 2×2 image mosaic.

We used the Amazon EC2 service with instance type c5.9xlarge [1] as our environment. This instance type was selected for having a guaranteed 10 Gbps network bandwidth in a shared network, and each instance provides 36 vCPUs (18 physical cores). We make use of a single instance type c5.24xlarge, which has 96 vCPUs and a guaranteed 25 Gbps network bandwidth for our experiments with clusters of heterogeneous nodes. Julia CMM was developed on version 1.0 of the Julia language.

Table 4 demonstrates the accuracy of the simulation is comparable with the execution of the benchmarks, with predicted values usually comprising a 5–20 % difference from actual values. The simulation thereby is at a point where its time-model prediction is useful in effective task scheduling, particularly with the average simulation time being less than 0.2 s acting as a marginal overhead. There is overhead in managing the task dependencies during execution, causing the node-level tile cache to be slightly underestimated in the simulation, contributing to the slight accuracy deviation.

As depicted in Table 5, with too small tile sizes, the communication overhead from more tasks is large enough to slow the benchmark down. However, the performance sharply degrades from 5 k to 7 k tile sizes for all benchmarks. With too large tile sizes, not enough parallelism takes place in the framework. As most benchmarks see their best performance in the 5 k tile size range, all results are presented with a default tile size of 5 k. This comparison uses simulation times, as we have shown that the accuracy of simulation is comparable with execution in Table 4.

Figure 2 shows the results of scheduling tasks for the Markov benchmark with an increasing number of nodes in the network. The memory allocation tasks `malloc` are scheduled first on each node followed by data initialization tasks `fillzero`. Communication tasks are split into `send` on the sender’s side and `recv` on the receiver’s side. Matrix addition and multiplication take place in computation tasks

Table 4. Julia CMM performance for matrix sizes of 10 k to 30 k, at a tile size of 5 k, for heterogeneous clusters of up to 14 nodes averaged over 20 runs. Each cluster has one AWS c5.24xlarge instance as the master node, and AWS c5.9xlarge as the remaining nodes. "Execution Time" depicts the execution times, "Speedup" depicts the relative speedup, "Predicted Time" depicts the execution time predicted by the simulation, and "Accuracy" depicts the accuracy of the prediction. The geometric mean of the relative speedups across all benchmarks is depicted at the bottom.

Name	Nodes	Execution Time (s)					Speedup (x)					Predicted Time (s)					Accuracy (%)				
		10k	15k	20k	25k	30k	10k	15k	20k	25k	30k	10k	15k	20k	25k	30k	10k	15k	20k	25k	30k
Markov	1	6.39	12.52	17.67	20.23	24.58	1.00	1.00	1.00	1.00	1.00	5.80	11.91	17.41	19.86	23.65	110	105	102	102	104
	2	5.41	9.64	13.84	15.51	17.03	1.18	1.30	1.28	1.30	1.44	4.62	9.48	13.37	15.28	16.88	117	102	103	102	101
	4	3.49	7.16	12.29	14.25	15.96	1.83	1.75	1.44	1.42	1.54	3.30	6.25	12.05	13.83	15.44	106	115	102	103	103
	6	2.59	6.07	11.42	11.42	13.33	2.47	2.06	1.55	1.77	1.84	2.27	4.97	10.41	9.62	10.99	114	122	111	119	121
	8	2.22	6.87	10.60	10.49	11.09	2.88	1.82	1.67	1.93	2.22	1.76	6.70	10.51	8.96	10.88	126	103	101	117	102
	10	1.82	5.54	9.19	9.31	9.22	3.51	2.26	1.92	2.17	2.67	1.55	5.06	8.25	8.71	8.33	118	110	111	107	111
	12	1.52	5.09	7.29	7.74	8.82	4.22	2.46	2.43	2.61	2.79	1.24	4.31	6.88	6.60	8.50	122	118	106	117	104
	14	1.28	4.60	6.93	6.73	7.89	4.99	2.72	2.55	3.01	3.12	1.07	3.77	6.76	5.28	7.46	120	122	102	127	106
K-Means	1	10.09	14.45	18.95	23.89	26.14	1.00	1.00	1.00	1.00	1.00	9.34	13.83	18.20	23.05	25.56	108	105	104	104	102
	2	6.40	10.31	13.49	18.98	22.52	1.58	1.40	1.41	1.26	1.16	6.11	9.66	12.72	18.43	21.80	105	107	106	103	103
	4	5.18	12.00	13.65	14.77	16.27	1.95	1.20	1.39	1.62	1.61	5.14	11.25	13.30	14.43	15.75	101	107	103	102	103
	6	4.85	8.21	12.61	14.56	17.91	2.08	1.76	1.50	1.64	1.46	4.36	7.51	12.52	14.53	17.22	111	109	101	101	100
	8	2.94	7.39	11.00	12.49	15.80	3.44	1.96	1.72	1.91	1.65	2.79	7.25	10.25	11.64	15.74	105	102	107	107	100
	10	2.42	8.14	9.22	11.07	13.50	4.18	1.78	2.05	2.16	1.94	1.96	7.88	8.99	10.15	12.89	123	103	103	109	105
	12	2.00	6.11	9.91	11.76	12.39	4.59	2.37	1.91	2.03	2.11	2.07	5.44	9.61	11.36	12.37	116	112	103	104	100
	14	2.05	4.77	7.18	10.74	11.34	4.92	3.03	2.64	2.22	2.31	1.72	3.93	6.68	10.51	10.99	109	122	107	102	103
Hill	1	7.48	14.38	19.43	24.68	29.18	1.00	1.00	1.00	1.00	1.00	7.03	13.54	19.20	24.18	28.34	106	106	101	102	103
	2	6.15	9.07	15.67	15.59	22.33	1.22	1.59	1.24	1.58	1.31	5.33	8.48	15.13	15.52	21.81	116	107	104	100	102
	4	3.60	9.73	14.26	17.13	18.78	2.08	1.48	1.36	1.44	1.55	3.16	8.75	14.15	16.30	17.84	114	111	101	105	105
	6	3.21	5.64	11.71	14.26	15.33	2.33	2.55	1.66	1.73	1.90	2.88	4.75	11.30	13.75	14.36	112	119	104	104	107
	8	2.73	6.89	11.19	12.49	14.82	2.74	2.09	1.74	1.98	1.97	2.61	6.27	10.66	11.83	14.09	105	110	105	106	105
	10	2.68	4.50	10.49	10.56	13.51	2.80	3.20	1.85	2.34	2.16	2.38	3.77	10.06	9.90	13.42	112	119	104	107	101
	12	2.19	3.88	8.72	9.31	13.16	3.42	3.70	2.23	2.65	2.22	1.74	3.41	8.47	8.67	12.89	125	114	103	107	102
	14	1.81	3.19	7.58	8.76	12.27	4.13	4.51	2.56	2.82	2.38	1.45	2.70	6.81	7.84	11.39	125	118	111	112	108
Leontief	1	10.51	17.31	22.08	26.66	32.13	1.00	1.00	1.00	1.00	1.00	10.43	16.48	21.93	26.65	31.33	101	105	101	100	103
	2	9.34	12.40	18.27	21.45	23.98	1.13	1.40	1.21	1.24	1.34	8.88	12.29	18.05	21.17	23.15	105	101	101	101	104
	4	8.24	11.81	17.19	17.47	18.79	1.28	1.47	1.28	1.53	1.71	8.23	10.88	16.91	17.42	17.92	100	109	102	100	105
	6	7.47	8.91	15.03	16.36	16.75	1.41	1.94	1.47	1.63	1.92	7.07	8.81	14.50	15.41	15.87	106	101	104	106	106
	8	6.38	8.27	15.28	16.52	15.39	1.65	2.09	1.45	1.61	2.09	6.31	7.83	14.68	16.38	15.16	101	106	104	101	101
	10	5.58	8.58	14.07	13.43	14.35	1.89	2.02	1.57	1.99	2.24	5.09	8.58	13.93	12.93	14.18	110	100	101	104	101
	12	5.15	6.00	12.28	14.95	12.46	2.04	2.89	1.80	1.78	2.58	4.77	5.39	11.74	14.40	12.04	108	111	105	104	104
	14	4.66	5.89	12.40	14.19	11.56	2.26	2.94	1.78	1.88	2.78	4.24	5.52	11.53	13.78	11.12	110	107	108	103	104
Synth	1	7.87	12.38	19.43	27.53	34.78	1.00	1.00	1.00	1.00	1.00	6.71	12.32	18.57	27.23	34.04	117	101	105	101	102
	2	5.86	10.28	13.71	23.80	24.47	1.34	1.20	1.42	1.16	1.42	5.06	9.38	12.90	23.37	24.13	116	110	106	102	101
	4	4.73	9.16	13.21	19.26	22.07	1.66	1.35	1.47	1.45	1.58	4.66	8.40	12.72	19.17	21.15	102	109	104	100	104
	6	3.98	6.36	11.57	17.63	20.19	1.98	1.89	1.68	1.56	1.72	3.72	5.66	10.88	17.61	19.17	107	116	104	100	104
	8	3.60	8.38	9.50	14.72	18.89	2.19	2.30	2.04	1.87	1.84	2.83	4.82	9.08	14.40	18.58	127	112	105	103	102
	10	3.08	4.96	8.79	13.54	17.92	2.55	2.50	2.21	2.03	1.94	2.89	4.00	8.54	13.21	17.88	115	124	103	102	100
	12	2.86	4.36	8.50	10.74	16.01	2.75	2.84	2.28	2.56	2.17	2.76	3.93	8.18	10.32	15.41	104	111	104	104	104
	14	2.75	4.14	8.00	9.78	13.84	2.86	2.99	2.43	2.82	2.51	2.32	4.07	7.63	9.01	12.91	118	102	105	109	107
Reachability	1	9.70	16.78	21.89	24.96	34.04	1.00	1.00	1.00	1.00	1.00	9.57	16.76	21.17	24.16	33.47	101	100	103	103	102
	2	8.44	13.09	18.50	20.23	27.01	1.15	1.28	1.18	1.23	1.26	8.36	12.69	17.67	19.77	26.33	101	103	105	102	102
	4	7.11	12.27	18.05	18.67	24.99	1.36	1.37	1.21	1.34	1.36	6.62	11.30	17.07	17.73	24.16	107	109	106	105	103
	6	6.66	12.18	17.95	17.67	20.18	1.46	1.38	1.22	1.41	1.69	6.26	11.84	17.75	16.81	19.33	106	103	101	105	104
	8	5.86	10.17	14.72	16.81	19.64	1.66	1.65	1.49	1.48	1.73	4.97	9.93	14.21	16.66	19.62	118	102	104	101	100
	10	5.79	9.72	12.08	14.20	18.30	1.68	1.73	1.81	1.76	1.86	5.77	9.22	11.83	13.91	17.62	100	106	102	102	104
	12	4.91	9.42	11.88	13.07	18.17	1.98	1.78	1.84	1.91	1.87	4.29	9.38	11.25	12.88	17.30	115	100	106	101	105
	14	4.26	7.96	10.33	11.53	15.76	2.28	2.11	2.12	2.16	2.16	3.61	6.99	9.96	11.34	15.73	118	114	104	102	100
Hits	1	9.86	15.22	21.94	30.61	38.95	1.00	1.00	1.00	1.00	1.00	8.90	14.82	21.81	30.38	38.26	111	103	101	101	102
	2	7.30	13.84	17.83	25.68	30.32	1.35	1.10	1.23	1.19	1.28	6.89	13.04	16.83	25.66	29.73	106	106	106	100	102
	4	6.56	10.69	17.63	20.72	25.76	1.50	1.42	1.24	1.48	1.51	5.57	9.73	17.17	20.66	25.57	118	110	103	100	101
	6	6.47	10.22	16.69	20.51	22.09	1.52	1.49	1.31	1.49	1.76	5.84	9.64	15.85	19.86	21.74	111	106	105	103	102
	8	5.42	9.34	16.27	17.95	21.80	1.82	1.63	1.35	1.71	1.79	4.68	9.06	15.36	17.91	21.06	116	103	106	100	104
	10	4.37	9.00	11.86	16.50	19.25	2.26	1.69	1.85	1.86	2.02	3.83	8.35	11.53	16.17	18.29	114	108	103	102	105
	12	4.32	8.36	11.27	15.85	18.28	2.28	1.82	1.95	1.93	2.13	4.14	7.95	10.63	15.05	17.77	104	105	106	105	103
	14	4.23	8.31	10.51	14.20	18.50	2.33	1.83	2.09	2.16	2.10	3.78	8.19	9.76	14.08	17.83	112	102	108	101	104
BFS	1	22.27	31.92	49.40	73.04	104.88	1.00	1.00	1.00	1.00	1.00	21.80	31.20	48.90	72.89	104.61	102	102	101	100	100
	2	20.14	24.03	36.26	49.86	71.27	1.11	1.33	1.36	1.46	1.47	19.95	23.04	35.92	49.09	70.36	101	104	101	102	101
	4	16.67	20.19	29.93	38.50	57.82	1.34	1.58	1.65	1.90	1.81	15.69	20.13	29.22	37.51	57.45	106	100			

Table 5. Comparison of simulated execution times at different tile sizes for the Markov benchmark. The profiled data was obtained from eight AWS c5.9x large instances (nodes) at a matrix size of 10 k, and the average over 20 runs per tile size is stated.

Name	Nodes	Tile size																		
		500	1k	1.5k	2k	2.5k	3k	3.5k	4k	4.5k	5k	5.5k	6k	6.5k	7k	7.5k	8k	8.5k	9k	9.5k
Markov	1	11.24	10.20	9.25	8.86	7.73	7.71	7.42	6.95	6.07	5.03	6.26	8.14	13.06	20.76	21.23	21.60	22.60	22.95	22.98
	2	7.75	4.92	4.74	4.60	4.42	3.61	3.26	3.12	3.28	2.67	4.13	6.46	8.65	12.69	13.58	13.92	15.19	17.09	17.17
	4	6.05	4.14	3.27	2.94	3.09	2.81	2.87	2.42	2.30	1.96	2.45	3.21	6.68	11.35	12.67	13.48	14.52	16.39	17.17
	6	6.22	4.48	3.49	3.48	3.33	3.26	2.78	1.79	1.75	1.39	1.62	1.84	8.40	10.14	11.75	12.32	12.86	13.19	13.67
	8	4.65	3.77	3.44	3.10	3.25	2.92	2.39	1.39	1.24	1.27	1.63	1.23	4.44	10.23	11.47	11.98	13.94	14.42	14.67
Kmeans	1	14.13	10.86	11.25	10.25	10.32	9.08	7.41	6.15	5.77	4.52	7.15	8.63	12.87	18.43	19.81	20.00	20.95	21.66	22.34
	2	8.13	6.85	6.51	6.46	5.38	3.80	4.18	4.33	4.06	4.10	5.50	5.73	7.52	11.17	12.94	13.72	15.23	16.04	17.03
	4	8.10	4.72	5.20	4.82	4.10	3.44	3.92	3.05	3.55	3.62	4.49	4.99	5.75	9.58	10.52	11.04	11.48	13.41	14.32
	6	7.08	4.84	4.04	3.60	3.42	3.63	2.90	3.05	3.24	2.51	2.45	2.59	4.65	7.68	9.23	10.21	11.82	12.07	12.89
	8	4.55	3.74	3.02	2.62	2.68	2.34	1.85	1.73	1.73	1.37	1.65	3.90	5.10	7.43	7.84	8.63	8.72	9.61	10.20
Hill	1	13.04	10.17	10.37	9.95	8.32	7.90	6.99	6.36	5.38	4.76	7.03	8.82	11.50	17.86	18.65	19.33	20.43	21.34	21.61
	2	7.71	6.36	5.40	5.08	4.47	3.85	3.84	3.66	2.93	2.30	3.69	3.99	9.22	11.80	12.81	12.88	13.15	13.87	14.20
	4	6.22	5.35	4.92	3.55	3.20	3.44	2.70	2.54	2.74	2.10	3.20	4.49	6.99	9.42	9.89	10.23	11.85	12.67	12.78
	6	5.73	5.15	4.14	3.79	3.45	3.19	2.80	2.77	2.20	1.28	2.50	2.60	7.92	9.39	9.43	10.25	11.08	12.41	12.60
	8	4.76	3.78	3.79	3.66	2.85	2.81	1.93	1.61	1.05	0.86	1.49	4.70	5.95	9.92	10.45	10.71	11.83	12.71	13.53
Leontief	1	15.51	13.88	14.05	13.09	12.18	11.90	10.30	9.43	8.51	7.20	8.29	11.70	14.83	21.83	23.59	24.30	25.20	26.60	26.81
	2	11.34	9.70	9.57	9.39	8.17	7.78	8.15	8.01	7.50	6.98	8.20	9.45	13.47	15.81	16.66	16.96	18.92	19.06	19.39
	4	9.96	7.19	7.42	7.22	6.14	5.76	5.40	5.25	5.34	5.32	6.66	7.56	9.77	13.86	15.26	16.00	17.76	18.78	19.25
	6	9.28	7.07	6.41	6.39	6.39	6.45	5.68	5.47	4.81	3.96	3.74	5.37	11.40	12.56	12.63	12.86	13.12	13.60	14.58
	8	6.21	6.58	5.98	5.77	5.66	5.05	4.91	4.23	3.30	3.01	3.59	4.74	9.54	11.77	12.01	12.28	13.51	14.94	15.89
Synth	1	13.60	10.76	10.61	10.28	9.95	8.60	8.05	6.32	4.40	3.52	6.63	8.70	12.65	16.83	17.67	18.13	19.16	19.87	20.30
	2	7.22	6.47	5.86	5.43	5.32	4.73	4.57	3.74	3.20	3.82	5.28	3.98	5.13	12.69	13.67	14.39	15.68	16.72	16.78
	4	7.42	6.36	4.65	4.56	4.04	4.10	4.05	3.30	3.17	3.58	3.96	6.44	6.31	11.82	13.66	14.45	15.22	15.47	15.51
	6	6.10	4.33	3.78	3.53	3.63	3.02	2.80	1.96	1.94	1.22	2.42	3.52	5.94	10.44	12.25	12.85	13.21	14.65	15.59
	8	3.65	3.97	3.12	3.17	2.83	3.09	2.52	1.67	1.21	0.80	1.44	2.58	5.43	11.60	12.41	13.03	14.54	14.74	15.13
Reachability	1	14.97	13.04	13.31	13.34	12.11	11.00	10.50	10.50	9.32	7.04	8.77	10.43	15.92	21.02	21.10	22.07	22.54	23.48	24.03
	2	10.51	8.69	8.08	7.54	7.56	8.33	7.54	7.67	7.72	6.24	6.74	7.22	13.59	16.08	16.43	16.80	17.79	18.46	19.26
	4	9.56	7.78	7.07	6.82	7.13	6.59	6.45	6.02	6.07	6.25	6.86	7.52	10.25	14.60	15.05	15.13	16.24	17.37	17.65
	6	9.12	7.24	6.51	6.19	6.45	6.00	4.39	4.60	4.95	4.83	6.98	5.21	8.52	13.99	14.76	14.92	16.71	17.98	18.09
	8	6.63	5.94	6.14	5.67	4.98	4.94	3.76	3.62	3.82	3.19	5.55	6.74	10.36	13.21	14.98	15.12	15.65	17.43	17.71
Hits	1	16.56	14.85	13.66	13.32	12.30	11.70	10.91	10.37	9.35	8.70	9.18	9.73	15.31	21.49	22.47	22.71	24.28	24.89	25.88
	2	11.15	9.24	8.44	8.57	7.12	6.99	7.61	6.86	6.46	5.98	6.26	7.86	10.22	16.69	18.13	19.13	19.84	21.65	22.54
	4	10.49	8.51	7.31	7.32	6.89	7.78	6.23	6.21	5.14	4.94	5.67	7.34	9.34	14.92	15.77	16.62	17.24	18.42	18.64
	6	9.53	7.04	6.72	6.59	6.09	6.16	4.62	4.90	4.80	4.34	4.77	8.38	9.76	13.90	14.95	15.41	15.62	15.80	15.92
	8	7.68	5.83	5.88	5.32	4.69	3.27	3.48	3.01	3.25	2.62	3.53	3.09	9.23	10.28	10.57	11.13	11.62	12.73	13.67
Parboil-BFS	1	34.83	33.30	30.20	29.15	25.74	23.42	22.90	22.54	21.43	20.46	23.23	25.67	29.71	30.38	31.97	34.45	37.19	37.28	39.31
	2	29.16	27.31	23.26	23.73	23.99	22.22	21.80	20.02	19.62	18.55	19.16	20.50	22.04	24.92	27.84	30.23	30.93	37.53	38.60
	4	25.72	21.10	21.49	19.99	19.37	18.17	18.37	16.25	15.40	14.09	16.47	19.88	19.05	24.15	25.69	24.35	27.22	29.26	30.49
	6	23.38	18.08	18.85	18.03	17.21	16.85	16.22	15.84	12.57	12.59	14.29	15.64	17.32	21.37	22.31	23.01	23.37	24.40	27.76
	8	19.64	15.88	13.22	14.66	12.84	11.38	10.45	10.34	8.68	6.30	11.77	11.32	15.85	16.90	17.18	18.69	20.61	22.04	20.78
Parboil-MM	1	45.98	41.13	39.46	38.32	38.49	35.11	34.27	33.72	30.98	28.34	35.34	35.59	36.98	36.69	39.48	44.77	45.62	46.57	47.13
	2	41.95	36.91	35.87	34.36	34.00	31.93	28.94	28.13	27.88	23.47	29.62	30.43	31.24	33.00	34.72	37.47	40.46	45.33	51.85
	4	36.48	28.19	27.22	27.73	27.11	25.16	25.23	24.31	22.20	19.72	23.27	25.58	27.86	35.24	35.08	37.52	37.90	37.51	42.41
	6	32.83	28.29	26.73	27.46	26.40	25.06	22.11	21.13	19.77	17.30	20.39	23.12	25.25	28.95	28.79	27.60	31.15	31.09	37.73
	8	28.64	21.90	21.68	19.87	19.24	17.50	16.97	15.52	13.85	10.77	15.23	18.69	20.84	21.93	22.81	23.57	25.91	28.71	28.52
Parboil-SPMV	1	61.91	52.10	52.87	49.14	48.80	47.02	44.35	42.15	41.21	36.69	36.53	40.58	43.91	47.94	49.83	49.17	52.94	55.01	64.30
	2	49.33	43.05	42.35	41.94	40.81	37.09	35.96	34.75	31.46	27.14	29.70	31.59	32.78	39.81	40.21	42.58	48.82	52.81	58.16
	4	50.98	43.59	42.87	41.85	41.18	39.27	36.08	32.24	27.62	25.85	35.28	35.70	36.35	37.80	39.65	40.34	41.78	44.19	47.73
	6	47.59	40.75	37.56	36.60	34.49	30.36	30.71	28.86	24.18	22.02	34.58	35.50	34.71	34.86	36.50	36.69	43.29	45.24	48.75
	8	36.20	34.64	33.99	33.34	30.51	29.83	29.68	22.42	18.45	14.78	21.00	21.34	26.89	26.81	28.15	33.70	35.60	39.73	42.59
Montage	1	96.15	81.31	85.11	84.38	80.53	75.44	69.87	66.05	63.74	58.50	63.84	78.31	78.83	80.60	86.67	88.37	86.77	95.35	95.82
	2	88.53	75.30	73.81	71.66	68.28	63.14	62.03	59.44	48.86	41.89	58.88	61.01	66.05	73.28	72.28	75.77	79.60	80.29	87.35
	4	90.48	85.39	79.02	74.91	69.35	68.05	63.92	52.45	45.62	37.89	61.34	68.35	69.14	70.98	71.08	70.35	73.60	73.36	81.59
	6	81.23	74.62	73.44	63.17	51.69	48.60	37.84	32.70	28.87	22.20	42.51	54.33	61.02	63.16	66.30	71.94	75.25	77.37	81.55
	8	77.83	64.69	60.62	54.24	47.42	42.21	37.21	31.79	22.77	16.63	39.39	56.47	61.48	63.58	68.17	65.29	69.84	73.94	76.09

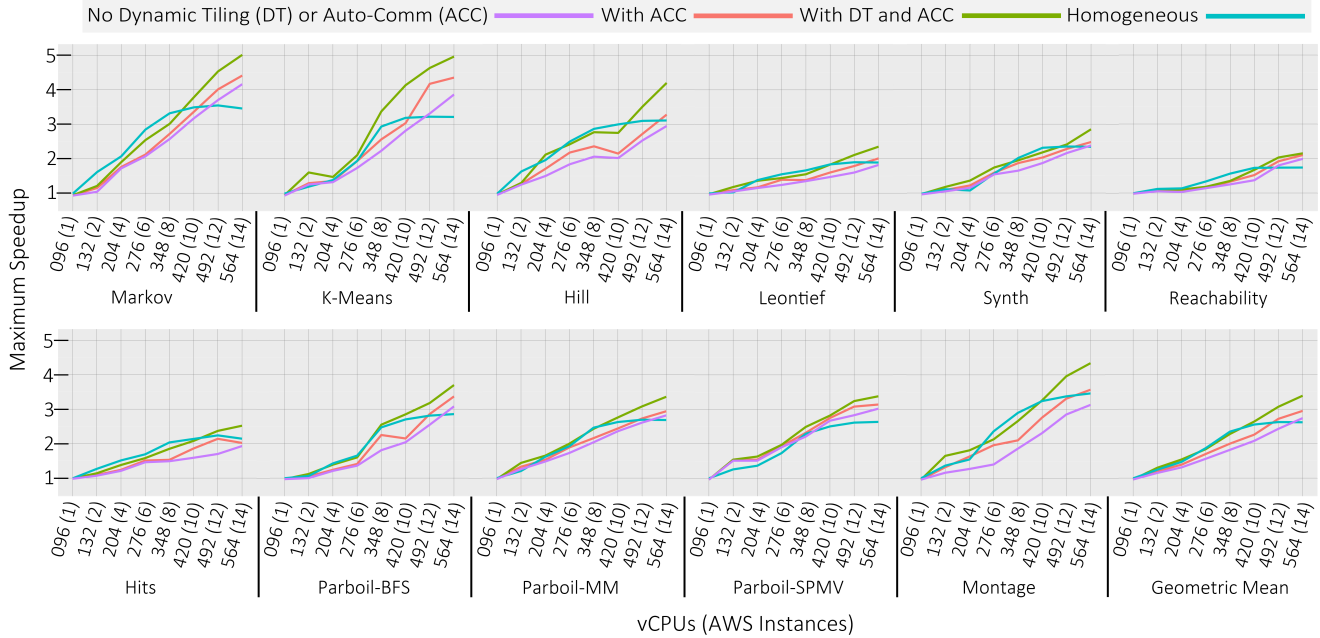


Figure 4. Julia CMM speedups without any optimizations, with the automatic communicator configuration (ACC), and with both ACC and dynamic tiling, on a heterogeneous network of one c5.24xlarge AWS instance node (96 vCPUs) to up to fourteen nodes with c5.9xlarge AWS instances (564 vCPUs total). Julia CMM (the entire computation, including online simulation) is compared against the time to execute the benchmark in vanilla Julia on a single node. The homogeneous line shows the time to execute on a homogeneous network of c5.9xlarge AWS instances. Its x-axis values differ by the number of vCPUs, in that they go from 036(1) to 288(8) in intervals of 36. All benchmarks were run with a matrix size of 10k, with simulated tile sizes ranging from 1k to 5k. The tile size that resulted in the highest performance in the online simulation is automatically selected by the framework. The last diagram depicts the geometric mean across all benchmarks.

admul!. Finally, takecopy! copies data from worker nodes into the master for the final matrix computation.

Figure 2a depicts a network with just the master and one worker node, and the schedule contains a total of 421 CMM tasks. Communication is sparse with the low number of nodes, being dominant at the beginning (sending data to the worker node) and at the end (receiving data from the worker node). Thus, only two communication processes in the master are sufficient to ensure load balance. With more nodes, as depicted in Figure 2b, two communication processes in the master are insufficient to ensure a balanced workload across the network. Processes would be busy to schedule new communication requests in a timely fashion, and there is a higher number of tasks to schedule, with 579 CMM tasks in the depicted schedule. Adding communication processes in the master thereby improves load balance by allowing communication requests to be finished earlier. However, it is naive to add an arbitrary number of communicators, as too many causes network contention by saturating the network with excess requests, worsening the latency of individual send operations. In such a scenario, the framework prefers utilizing the node-level tile cache in “seeded” nodes over sending matrix suboperations to new nodes. In all schedules, the first tasks on worker nodes are scheduled after the

first tasks on the master node because no communication is needed to schedule on the latter. Thus, with larger networks, the length of the startup phase is made more prominent.

Figure 4 depicts the maximum speedups of eleven benchmarks from one c5.24xlarge AWS instance (96 vCPUs) to fourteen nodes extended with c5.9xlarge AWS instances (564 vCPUs). Most maximum speedups exceed $2\times$, with some reaching $5\times$. The Markov benchmark reaches a speedup of $5.01\times$ with the best performing tile size, and the Montage benchmark reaches $4.34\times$ maximum speedup compared to vanilla Julia. For all configurations, performance improves with dynamic tiling, as it helps to mitigate the communication bottleneck. Dynamic tiling ensures all workers are active, and the node-level tile cache ensures they remain active, improving performance particularly with higher node counts.

Table 4 demonstrates the framework’s scalability at larger matrix sizes within the same benchmark and network parameters, with comparable results still obtainable at benchmarks of a larger size without significant failure points, as a result of the dynamic tiling optimization encouraging the usage of all nodes in parallelizing larger matrices. A consistent trend amongst all benchmarks is that with increasing network size, the benchmark performance improves as a result. However,

as reflected in Figure 4, the degree of improvement slows down at ≥ 10 nodes in most benchmarks when working with a homogeneous cluster, where minimal speedup improvement is obtained from adding more nodes. This is the result of the limited number of communication processes available in the master node, which did not scale up with the network size. Thus, additional nodes compete with existing nodes for receiving data from the master node albeit its limited number of communication processes. The dynamic tiling optimization is ineffective, where after the startup phase in an excessively large network, the master node is unable to efficiently distribute data to all worker nodes without experiencing significant stalls in the worker nodes.

Thus, we present the performance of dynamic tiling and auto-communication configuration on a non-homogeneous cluster where the master node is significantly more powerful than the worker nodes, and thereby contains more communication processes. At higher node counts in the cluster, the performance improvement obtained with the heterogeneous configuration is $\geq 40\%$, and goes up to 150% . Likewise, we find that the declining performance improvement gains with larger network sizes is not as prevalent with a stronger master node, as depicted in Figure 4. This is the result of the greater communication capacity allowing for more inter-node communication to take place, and when coupled with dynamic tiling, facilitates higher inter-node communication bandwidth. We find that the performance improvement is substantial over the homogeneous cluster, which is to be expected due to the communication being less of a bottleneck.

We note that with heterogeneous networks, both speedups for with and without dynamic tiling generally exhibit a linear pattern with a gradual performance drop at higher node counts. We observed that the speedup improvement gained with dynamic tiling for the tested heterogeneous network is generally not as large as the improvement gained in a homogeneous network of $c5.9x$ large AWS instances. However, as the heterogeneous configuration is question was created to mitigate communication limitations, this is to be expected. We note that the dynamic tiling’s effectiveness is more apparent at higher node counts which require higher communication costs. Furthermore, the improvement in performance with just the automatic communicator configuration as opposed to vanilla Julia indicates that with minimal user input, the framework is capable of automatically configuring a given cloud network such that it reduces communication latency between potentially disparate nodes. With the inclusion of dynamic tiling, both optimizations help to reduce the effect of communication latency on an application’s potential performance.

Table 6 demonstrates the performance improvement from the dynamic tiling optimization. For ≥ 2 nodes in most benchmarks, it results in a $\geq 10\%$ speedup. The improvement is most apparent with Montage at 276% , which is due to it already being structured as a workflow that is flexible to

dynamic tile sizes. We observe a general trend that with increasing input matrix size, the performance improvement with the optimization gradually decreases. This can be attributed to the tile size of $5k$ comprising a smaller portion of a larger matrix, and thus not affecting the overall schedule as much. A large starting tile size in a larger matrix size of $20k$ results in longer individual tasks to schedule, which does not scale well with the optimization.

Table 8 depicts the performance gain achieved with all the matrix algebraic optimizations applied during the tree rewriting stage. We find that the speedup achieved is not insignificant, with most speedups being $\geq 10\%$ to as high as 50% , thereby demonstrating the effectiveness of the optimizations. We find that the time spent conducting the optimizations at runtime is generally on the order of milliseconds, which is comparatively insignificant to the overall time spent executing the entire benchmark, and thereby does not adversely affect the performance.

Table 9 demonstrates the time it takes to run a Markov benchmark with varying configurations of communicator and worker processes in the master node. We find that there is a trend of worsening performance with reducing the number of communicators while keeping the same number of workers, which is expected as less data is able to be propagated to worker nodes in the same amount of time. We find that increasing the number of workers usually improves the performance then degrades after a certain point. This occurs by introducing too many worker processes in the master node, causing the framework to favor scheduling tasks there due to its zero communication cost. Finally, we find that allocating less communicators with more workers can achieve a higher performance result than allocating the maximum number of communicator processes permissible by the bandwidth limit, and then filling the remaining cores with worker processes. We find that when working with a 10 Gbps bandwidth network, we can allocate up to 14 communicators in the master node before network saturation is detected, as indicated in Table 10. In Table 9, the performance achieved with 2 or 3 worker processes in the master is consistently weaker than with 4 worker processes, even when allocating the maximum number of communicators. This demonstrates that focusing only on communication awareness is naive, and the availability of computational resources should additionally be taken into account. Thus, instead of adhering to simply to maximizing communication capability, we aim to balance the two amounts according to the resources available on the master node.

By Amdahl’s Law, we calculate the upper bound of the speedups that is attainable with an infinitely fast network by setting communication latency to zero in the simulation. Other parameters remain the same: eight nodes with a matrix size of $10k$ and tile size of $5k$. As all tasks are parallelizable and asynchronous, communication acts as the bottleneck to true parallelism. Table 7 shows that with dynamic tiling,

most benchmarks do not significantly deviate from the upper bound, being in the range of 9–43 % from the upper bound. This is expected, as the upper bound is practically infeasible due to necessitating instantaneous communication.

5 Conclusions

We proposed the CMM framework which extends the Julia language to automatically parallelize matrix computations for the cloud with minimal user intervention. The framework employs offline profiling to generate accurate time prediction models using polynomial regression. They are used with tiled dependencies by the modified HEFT scheduler to allocate tasks such that overall execution time is minimized. Communication overhead optimizations are made by introducing additional communication processes, dynamic tiling, and the node-level tile cache. The implementation of an automatic communication configuration allowing the transition to heterogeneous clusters led to improvements in reducing the effect of communication overhead. We conducted an extensive experimental evaluation on a set of benchmarks using up to fourteen nodes (564 vCPUs) in the AWS public cloud. Our framework achieved speedups of up to a factor of 5.1, with an average 74.39 % of the upper bound for speedups.

Table 6. Performance improvement of the dynamic tiling optimization for matrix sizes of 10 k, 15 k, and 20 k, at a tile size of 5 k. The columns depict the original simulated execution time, the improved one with dynamic tiling alone and no other optimizations, and the relative speedup compared to without the optimization. The geometric mean of the speedups for all 11 benchmarks are listed at the end.

Name	Nodes	Original (s)			Optimized (s)			Speedup (×)		
		10k	15k	20k	10k	15k	20k	10k	15k	20k
Markov	1	6.15	11.99	17.38	6.04	11.91	16.81	1.02	1.01	1.03
	2	4.80	10.49	15.97	2.97	9.10	14.46	1.61	1.15	1.10
	4	4.17	8.74	14.54	2.86	7.79	13.09	1.46	1.12	1.11
	6	3.00	7.63	14.24	1.79	6.43	12.64	1.67	1.19	1.13
	8	2.60	7.83	13.34	1.57	6.45	11.66	1.66	1.21	1.14
Kmeans	1	7.64	13.62	18.23	7.55	13.18	18.23	1.01	1.03	1.00
	2	6.78	10.92	16.92	6.10	9.49	15.06	1.11	1.15	1.12
	4	5.58	10.09	16.27	5.12	9.17	14.04	1.09	1.10	1.16
	6	3.86	9.74	15.64	3.51	8.42	13.78	1.10	1.16	1.14
	8	2.51	7.70	13.81	2.37	6.80	11.63	1.06	1.13	1.19
Hill	1	6.39	12.25	17.59	6.12	11.85	17.43	1.04	1.03	1.01
	2	3.79	8.98	15.02	3.30	8.10	13.80	1.15	1.11	1.09
	4	3.28	8.98	14.81	2.80	7.92	13.42	1.17	1.13	1.10
	6	2.06	7.66	13.99	1.78	6.63	12.02	1.16	1.15	1.16
	8	1.92	7.82	13.23	1.56	6.69	11.73	1.23	1.17	1.13
Leontief	11	10.06	15.58	21.22	9.50	15.09	20.63	1.06	1.03	1.03
	2	8.80	14.23	20.04	7.98	12.14	18.49	1.10	1.17	1.08
	4	6.73	12.27	18.35	6.32	10.31	15.37	1.06	1.19	1.19
	6	5.45	11.24	16.74	4.96	9.58	14.61	1.10	1.17	1.15
	8	4.43	9.50	16.43	4.01	7.90	14.71	1.11	1.20	1.12
Synth	1	6.08	11.92	17.58	5.84	11.76	17.26	1.04	1.01	1.02
	2	5.62	9.71	16.09	4.82	8.33	14.86	1.17	1.17	1.08
	4	6.16	10.07	15.17	4.58	9.03	13.52	1.34	1.12	1.12
	6	4.76	7.98	14.08	2.22	6.88	12.52	2.15	1.16	1.12
	8	3.34	6.56	12.57	1.40	5.49	11.08	2.38	1.19	1.13
Reachability	1	9.36	15.33	20.66	9.02	14.82	19.96	1.04	1.03	1.03
	2	7.42	13.17	19.00	7.24	11.57	17.22	1.02	1.14	1.10
	4	7.65	12.98	18.50	7.25	11.48	17.13	1.05	1.13	1.08
	6	7.05	11.68	17.09	6.83	10.72	15.00	1.03	1.09	1.14
	8	4.56	9.95	15.85	4.19	8.43	13.24	1.09	1.18	1.20
Hits	1	9.87	15.09	21.16	9.72	14.76	20.83	1.02	1.02	1.02
	2	7.49	12.93	19.09	6.98	11.44	17.60	1.07	1.13	1.08
	4	6.24	11.72	17.62	5.94	10.13	16.27	1.05	1.16	1.08
	6	5.67	10.84	16.92	5.34	9.02	14.98	1.06	1.20	1.13
	8	3.34	9.75	15.74	2.92	7.93	13.61	1.15	1.23	1.16
BFS	1	22.06	31.79	48.52	21.48	30.92	47.3	1.03	1.03	1.03
	2	20.43	27.19	45.07	18.55	23.49	35.44	1.10	1.16	1.27
	4	17.08	22.69	39.69	14.09	18.96	28.14	1.21	1.20	1.41
	6	15.54	19.15	37.41	12.59	16.97	21.84	1.23	1.13	1.71
	8	8.06	17.29	36.87	6.70	12.59	17.74	1.20	1.37	2.08
MM	1	33.12	47.51	71.62	31.92	46.56	69.82	1.04	1.02	1.03
	2	26.53	35.26	62.97	23.47	32.05	52.92	1.13	1.10	1.19
	4	23.24	34.84	59.38	19.72	22.17	40.06	1.18	1.57	1.48
	6	19.40	29.92	55.91	17.30	15.98	27.34	1.12	1.87	2.04
	8	12.90	28.93	47.05	10.77	12.64	19.27	1.20	2.29	2.44
SPMV	1	41.70	49.48	73.15	40.82	48.06	72.08	1.02	1.03	1.01
	2	34.47	40.35	68.36	27.14	37.12	51.23	1.27	1.09	1.33
	4	32.49	38.89	62.46	25.85	30.6	45.11	1.26	1.27	1.38
	6	37.29	39.24	55.33	22.02	24.66	38.89	1.69	1.59	1.42
	8	28.42	34.68	49.88	14.78	19.19	27.23	1.92	1.81	1.83
Montage	1	68.24	80.94	106.43	66.52	78.41	104.87	1.03	1.03	1.01
	2	60.06	77.13	97.66	41.89	60.81	76.22	1.43	1.27	1.28
	4	58.00	76.11	93.33	37.89	47.13	61.24	1.53	1.61	1.52
	6	61.76	73.1	89.38	22.20	32.29	47.89	2.78	2.26	1.87
	8	49.65	69.29	85.66	16.63	18.45	33.52	2.98	3.76	2.56
Geomean 11 benchm.	1	-	-	-	-	-	-	1.03	1.02	1.02
	2	-	-	-	-	-	-	1.33	1.15	1.16
	4	-	-	-	-	-	-	1.35	1.23	1.23
	6	-	-	-	-	-	-	1.62	1.32	1.33
	8	-	-	-	-	-	-	1.87	1.47	1.46

Table 7. Speedups for a configuration of eight nodes over one node at a matrix size of 10 k and a tile size of 5 k. The one node configuration utilizes the AWS c5.24xlarge instance, which acts as the master in the eight node configuration, with the remaining nodes being AWS c5.9xlarge. Observed speedups are without dynamic tiling. New speedups are calculated with dynamic tiling enabled. Upper bounds assume zero communication time. All speedups assume that other optimizations, including the automatic communicator configuration, are present.

Benchmark Name	Observed Speedup (×)	Dynamic Tiling (×)	Upper bounds (w/o comm.) (×)
Markov	3.41	4.99	5.39
Kmeans	3.57	4.92	5.48
Hill	3.32	4.13	4.71
Leontief	2.14	2.26	3.90
Synth	2.48	2.86	4.23
Reachability	1.74	2.28	3.96
Hits	1.84	2.33	3.95
BFS	2.39	3.11	3.40
MM	2.37	3.21	3.75
SPMV	1.55	3.35	3.84
Montage	2.42	4.25	5.12

Table 8. Demonstration of the impact of matrix algebraic optimizations on the performance of Julia CMM, with a matrix size of 10 k and a tile size of 5 k on a cluster of eight nodes, with the master node using an AWS c5.24x large instance and worker nodes using c5.9xlarge instances. The unoptimized time shows the performance with all algebraic optimizations disabled, the optimized time shows the performance with all optimizations enabled, the speedup column shows the relative speedup gained from algebraic optimizations, the optimizations column shows the total number of algebraic optimizations performed, and the rewriting time column shows the time spent rewriting the expression trees based on the optimizations to be done.

Name	Unoptimized Time (s)		Optimized Time (s)		Speedup (×)		Optimizations		Rewriting Time (s)	
	10 k	20 k	10 k	20 k	10 k	20 k	10 k	20 k	10 k	20 k
Markov	2.38	13.10	2.22	10.6	1.07	1.24	289	499	0.038	0.078
Kmeans	3.15	13.72	2.94	9.22	1.07	1.49	229	334	0.043	0.077
Hill	3.46	16.82	2.73	11.19	1.27	1.50	197	309	0.031	0.086
Leontief	7.40	19.52	6.38	15.28	1.16	1.28	87	166	0.024	0.055
Synth	4.47	11.37	3.6	9.5	1.24	1.20	110	230	0.043	0.047
Reachability	6.53	16.07	5.86	14.72	1.11	1.09	60	220	0.015	0.084
Hits	6.25	19.56	5.42	16.27	1.15	1.20	108	245	0.030	0.053
BFS	9.29	22.65	8.73	19.67	1.06	1.15	189	313	0.058	0.099
MM	15.93	25.05	13.16	21.72	1.21	1.15	195	874	0.064	0.094
SPMV	17.72	32.24	16.19	27.71	1.09	1.16	105	672	0.046	0.077
Montage	29.06	42.68	26.73	38.86	1.09	1.10	324	1067	0.075	0.122
Average	-	-	-	-	-	-	-	-	0.039	0.076

Table 9. Simulated makespan to run the Markov benchmark with a matrix size of 20 k and a tile size of 5 k, based on the number of communicator and worker processes in the master node for a 12-node cluster comprised of a master node (AWS c5.24xlarge instance) and c5.9xlarge instances for the worker nodes. The bandwidth of the c5.24xlarge instance has been limited to 10 Gbps to remain consistent with the c5.9xlarge instances. The number of worker processes in the master node ranges from 2–5, and the number of communicator processes from 4–14 at a stride of 2. Durations are averaged over a total of 20 runs.

		Simulated Makespan (s)			
Num. Workers:		2	3	4	5
Num. Comm.	14	9.02	7.85	6.39	7.47
	12	9.33	7.97	6.41	7.59
	10	9.56	8.26	6.45	7.98
	8	10.19	9.13	6.64	8.51
	6	10.87	9.98	6.89	9.02
4	11.89	10.34	7.18	9.42	

Table 10. The maximum number of communicator processes per maximum bandwidth limit before network bandwidth saturation is detected, based on the network bandwidth capacities offered by AWS C5 instances [1].

Bandwidth (Gbps)	Num. Comm.
10	14
15	18
20	22
25	24

References

- [1] 2023. *Amazon Web Services, EC2 C5 Instances*.
- [2] 2023. *Project Jupyter web site*.
- [3] R. C. Agarwal, F. G. Gustavson, and M. Zubair. 1994. A high-performance matrix-multiplication algorithm on a distributed-memory parallel computer, using overlapped communication. *IBM Journal of Research and Development* 38, 6 (1994), 673–681. <https://doi.org/10.1147/rd.386.0673>
- [4] Alfred V. Aho, Monica S. Lam, Ravi Sethi, and Jeffrey D. Ullman. 2006. *Compilers: Principles, Techniques, and Tools* (2nd ed.). Addison-Wesley Longman Publishing Co., Inc., USA.
- [5] Serguei Diaz Baskakov and Juan Gutierrez Cardenas. 2021. Source to source compiler for the automatic parallelization of JavaScript code. In *2021 IEEE XXVIII International Conference on Electronics, Electrical Engineering and Computing (INTERCON)*. IEEE, Lima, Peru, 1–4. <https://doi.org/10.1109/INTERCON52678.2021.9532645>
- [6] Austin R. Benson and Grey Ballard. 2015. A Framework for Practical Parallel Fast Matrix Multiplication. In *Proceedings of the 20th ACM SIGPLAN Symposium on Principles and Practice of Parallel Programming (San Francisco, CA, USA) (PPoPP 2015)*. ACM, New York, NY, USA, 42–53. <https://doi.org/10.1145/2688500.2688513>
- [7] G. Bruce Berriman and J. C. Good. 2017. The Application of the Montage Image Mosaic Engine to the Visualization of Astronomical Images. *Publications of the Astronomical Society of the Pacific* 129, 975 (2017), 1–15. <https://doi.org/10.1088/1538-3873/aa5456>
- [8] Jeff Bezanson, Alan Edelman, Stefan Karpinski, and Viral B Shah. 2017. Julia: A fresh approach to numerical computing. *SIAM review* 59, 1 (2017), 65–98. <https://doi.org/10.1137/141000671>
- [9] L Susan Blackford, Jaeyoung Choi, Andy Cleary, Eduardo D’Azevedo, James Demmel, Inderjit Dhillon, Jack Dongarra, Sven Hammarling, Greg Henry, Antoine Petit, et al. 1997. *ScaLAPACK users’ guide*. SIAM, PA, USA.
- [10] Ewa Deelman, Rafael Ferreira da Silva, Karan Vahi, Mats Rynge, Rajiv Mayani, Ryan Tanaka, Wendy R. Whitcup, and Miron Livny. 2021. The Pegasus workflow management system: Translational computer science in practice. *Journal of Computational Science* 52 (2021), 101200. <https://doi.org/10.1016/j.jocs.2020.101200>
- [11] James Demmel, Mark Hoemmen, Marghoob Mohiyuddin, and Katherine Yelick. 2008. Avoiding communication in sparse matrix computations. In *2008 IEEE International Symposium on Parallel and Distributed Processing*. IEEE, 1–12. <https://doi.org/10.1109/IPDPS.2008.4536305>
- [12] Jack J Dongarra. 2022. The evolution of mathematical software. *Commun. ACM* 65, 12 (2022), 66–72. <https://doi.org/10.1145/3554977>
- [13] J. J. Dongarra, Jeremy Du Croz, Sven Hammarling, and I. S. Duff. 1990. A Set of Level 3 Basic Linear Algebra Subprograms. *ACM Trans. Math. Softw.* 16, 1 (March 1990), 1–17. <https://doi.org/10.1145/77626.79170>
- [14] Jack J. Dongarra, Jeremy Du Croz, Sven Hammarling, and Richard J. Hanson. 1988. An Extended Set of FORTRAN Basic Linear Algebra Subprograms. *ACM Trans. Math. Softw.* 14, 1 (March 1988), 1–17. <https://doi.org/10.1145/42288.42291>
- [15] Juan J Durillo and Radu Prodan. 2014. Multi-objective workflow scheduling in Amazon EC2. *Cluster computing* 17, 2 (2014), 169–189. <https://doi.org/10.1007/s10586-013-0325-0>
- [16] Efstratios Gallopoulos, Bernard Philippe, and Ahmed H Sameh. 2016. *Parallelism in matrix computations* (1st ed.). Springer, Dordrecht, Netherlands. <https://doi.org/10.1007/978-94-017-7188-7>
- [17] Jonathan S Golan. 1995. *Foundations of Linear Algebra* (1st ed.). Springer, Dordrecht, Netherlands. https://doi.org/10.1007/978-94-015-8502-6_16
- [18] Robert Graves, Thomas H Jordan, Scott Callaghan, Ewa Deelman, Edward Field, Gideon Juve, Carl Kesselman, Philip Maechling, Gaurang Mehta, Kevin Milner, et al. 2011. CyberShake: A physics-based seismic hazard model for southern California. *Pure and Applied Geophysics* 168, 3 (2011), 367–381. <https://doi.org/10.1007/s00024-010-0161-6>
- [19] Sachi Gupta, Sailesh Iyer, Gaurav Agarwal, Poongodi Manoharan, Abeer D Algarni, Ghadah Aldehim, and Kaamran Raahemifar. 2022. Efficient prioritization and processor selection schemes for HEFT algorithm: A makespan optimizer for task scheduling in cloud environment. *Electronics* 11, 16 (2022). <https://doi.org/10.3390/electronics11162557>
- [20] Ashraf M Hemeida, SA Hassan, Salem Alkhalaf, MMM Mahmoud, MA Saber, Ayman M Bahaa Eldin, Tomonobu Senjyu, and Abdullah H Alayed. 2020. Optimizing matrix-matrix multiplication on Intel’s advanced vector extensions multicore processor. *Ain Shams Engineering Journal* 11, 4 (2020), 1179–1190. <https://doi.org/10.1016/j.asej.2020.01.003>
- [21] Raymes Khoury, Bernd Burgstaller, and Bernhard Scholz. 2011. Accelerating the Execution of Matrix Languages on the Cell Broadband Engine Architecture. *IEEE Transactions on Parallel and Distributed Systems* 22, 1 (2011), 7–21. <https://doi.org/10.1109/TPDS.2010.58>
- [22] Donald E. Knuth. 1997. *The Art of Computer Programming, Volume 2: Seminumerical Algorithms* (3rd ed.). Addison-Wesley Longman Publishing Co., Inc., USA.
- [23] Erwin Kreyszig, Herbert Kreyszig, and E. J. Norminton. 2011. *Advanced Engineering Mathematics* (tenth ed.). Wiley, Hoboken, NJ.
- [24] Boonhatai Kruekaew and Warangkha Kimpan. 2020. Enhancing of Artificial Bee Colony Algorithm for Virtual Machine Scheduling and Load Balancing Problem in Cloud Computing. *International Journal of Computational Intelligence Systems* 13 (2020), 496–510. Issue 1. <https://doi.org/10.2991/ijcis.d.200410.002>
- [25] Jin Ho Kwak and Sungpyo Hong. 2004. *Linear Algebra* (2nd ed.). Birkhäuser, Boston, MA. <https://doi.org/10.1007/978-0-8176-8194-4>
- [26] C. L. Lawson, R. J. Hanson, D. R. Kincaid, and F. T. Krogh. 1979. Basic Linear Algebra Subprograms for Fortran Usage. *ACM Trans. Math. Softw.* 5, 3 (Sept. 1979), 308–323. <https://doi.org/10.1145/355841.355847>
- [27] Jay Hwan Lee, Yeonsoo Kim, Yonghyun Ryu, Wasuwee Sodsong, Hyunjun Jeon, Jinsik Park, Bernd Burgstaller, and Bernhard Scholz. 2022. Julia Cloud Matrix Machine: Dynamic Matrix Language Acceleration on Multicore Clusters in the Cloud. <https://doi.org/10.48550/ARXIV.2205.07421> arXiv:2205.07421 [cs.DC]
- [28] Shigang Li, ChangJun Hu, JunChao Zhang, and Yunquan Zhang. 2015. Automatic tuning of sparse matrix-vector multiplication on multicore clusters. *Science China Information Sciences* 58 (06 2015). <https://doi.org/10.1007/s11432-014-5254-x>
- [29] Jonathan Livny, Hidayat Teonadi, Miron Livny, and Matthew K Waldor. 2008. High-throughput, kingdom-wide prediction and annotation of bacterial non-coding RNAs. *PLoS one* 3, 9 (2008), e3197. <https://doi.org/10.1371/journal.pone.0003197>
- [30] Junior Loff, Renato B. Hoffman, Dalvan Griebler, and Luiz G. Fernandes. 2021. High-Level Stream and Data Parallelism in C++ for Multi-Cores. In *Proceedings of the 25th Brazilian Symposium on Programming Languages (SBLP’21)*. ACM, New York, NY, USA, 41–48. <https://doi.org/10.1145/3475061.3475078>
- [31] Hadeer Mahmoud, Mostafa Thabet, Mohamed H. Khafagy, and Fatma A. Omara. 2022. Multiobjective Task Scheduling in Cloud Environment Using Decision Tree Algorithm. *IEEE Access* 10 (2022), 36140–36151. <https://doi.org/10.1109/ACCESS.2022.3163273>
- [32] Tania Malik, Vladimir Rychkov, and Alexey Lastovetsky. 2016. Network-aware optimization of communications for parallel matrix multiplication on hierarchical HPC platforms. *Concurrency and Computation: Practice and Experience* 28, 3 (2016), 802–821. <https://doi.org/10.1002/cpe.3609> arXiv:https://onlinelibrary.wiley.com/doi/pdf/10.1002/cpe.3609
- [33] Yukio Miyasaka, Akihiro Goda, Ashish Mittal, and Masahiro Fujita. 2020. Synthesis and Generalization of Parallel Algorithm for Matrix-vector Multiplication. *IPSS Transactions on System LSI Design Methodology* 13 (01 2020), 31–34. <https://doi.org/10.2197/ipsjtsldm.13.31>

- [34] Thi My Tuyen Nguyen, Yoosang Park, Jaeyoung Choi, and Raehyun Kim. 2020. Evaluating performance of Parallel Matrix Multiplication Routine on Intel KNL and Xeon Scalable Processors. In *2020 IEEE International Conference on Autonomic Computing and Self-Organizing Systems Companion (ACOSOS-C)*. IEEE, Washington, DC, USA, 42–47. <https://doi.org/10.1109/ACOSOS-C51401.2020.00027>
- [35] Yuyao Niu, Zhengyang Lu, Haonan Ji, Shuhui Song, Zhou Jin, and Weifeng Liu. 2022. TileSpGEMM: A Tiled Algorithm for Parallel Sparse General Matrix-Matrix Multiplication on GPUs. In *Proceedings of the 27th ACM SIGPLAN Symposium on Principles and Practice of Parallel Programming* (Seoul, Republic of Korea) (PPoPP '22). ACM, New York, NY, USA, 90–106. <https://doi.org/10.1145/3503221.3508431>
- [36] Björn ohansson and Emil Österberg. 2018. Algorithms for Large Matrix Multiplications: Assessment of Strassen’s Algorithm. <https://urn.kb.se/resolve?urn=urn:nbn:se:kth:diva-230742>.
- [37] R. Onn, A.O. Steinhardt, and A.W. Bojanczyk. 1991. The hyperbolic singular value decomposition and applications. *IEEE Transactions on Signal Processing* 39, 7 (1991), 1575–1588. <https://doi.org/10.1109/78.134396>
- [38] V. Priya, C. Sathiy Kumar, and Ramani Kannan. 2019. Resource scheduling algorithm with load balancing for cloud service provisioning. *Applied Soft Computing* 76 (2019), 416–424. <https://doi.org/10.1016/j.asoc.2018.12.021>
- [39] Wang Qian, Zhang Xianyi, and Zhang Yunquan. 2022. OpenBLAS: An Optimized BLAS Library. <https://www.openblas.net/>.
- [40] Ravi Reddy, Alexey Lastovetsky, and Pedro Alonso. 2009. HeteroP-BLAS: A set of Parallel Basic Linear Algebra Subprograms optimized for heterogeneous computational clusters. *Scalable Computing: Practice and Experience* 10, 2 (2009), 201–216.
- [41] Andreas Rosowski. 2019. Fast Commutative Matrix Algorithm. <https://doi.org/10.48550/arXiv.1904.07683> arXiv:1904.07683 [cs.DS]
- [42] Yassir Samadi, Mostapha Zbakh, and Claude Tadonki. 2018. E-HEFT: Enhancement Heterogeneous Earliest Finish Time algorithm for Task Scheduling based on Load Balancing in Cloud Computing. In *2018 International Conference on High Performance Computing Simulation (HPCS)*. IEEE, Orleans, France, 601–609. <https://doi.org/10.1109/HPCS.2018.00100>
- [43] Shigeyuki Sato and Hideya Iwasaki. 2011. Automatic Parallelization via Matrix Multiplication, In Proceedings of the 32nd ACM SIGPLAN Conference on Programming Language Design and Implementation (PLDI’11). *ACM SIGPLAN Notices*, 470–479. <https://doi.org/10.1145/1993498.1993554>
- [44] John A. Stratton, Christopher Rodrigrues, I-Jui Sung, Nady Obeid, Liwen Chang, Geng Liu, and Wen-Mei W. Hwu. 2012. *Parboil: A Revised Benchmark Suite for Scientific and Commercial Throughput Computing*. Technical Report IMPACT-12-01. University of Illinois at Urbana-Champaign, Urbana. <http://impact.crhc.illinois.edu/Shared/Docs/impact-12-01.parboil.pdf>.
- [45] Ian J Taylor, Ewa Deelman, and Dennis B et al Gannon. 2007. *Workflows for e-science: scientific workflows for grids*. Springer, London. <https://doi.org/10.1007/978-1-84628-757-2>
- [46] H. Topcuoglu, S. Hariri, and Min-You Wu. 2002. Performance-effective and low-complexity task scheduling for heterogeneous computing. *IEEE Transactions on Parallel and Distributed Systems* 13, 3 (2002), 260–274. <https://doi.org/10.1109/71.993206>
- [47] Jeffrey D. Ullman. 1975. NP-complete scheduling problems. *Journal of Computer and System sciences* 10, 3 (1975), 384–393. [https://doi.org/10.1016/S0022-0000\(75\)80008-0](https://doi.org/10.1016/S0022-0000(75)80008-0)
- [48] Robert A Van De Geijn and Jerrell Watts. 1997. SUMMA: Scalable universal matrix multiplication algorithm. *Concurrency: Practice and Experience* 9, 4 (1997), 255–274. [https://doi.org/10.1002/\(SICI\)1096-9128\(199704\)9:4<255::AID-CPE250>3.0.CO;2-2](https://doi.org/10.1002/(SICI)1096-9128(199704)9:4<255::AID-CPE250>3.0.CO;2-2)
- [49] Qian Wang, Xianyi Zhang, Yunquan Zhang, and Qing Yi. 2013. AUGEM: automatically generate high performance dense linear algebra kernels on x86 CPUs. In *SC’13: Proceedings of the International Conference on High Performance Computing, Networking, Storage and Analysis*. IEEE, Denver, Colorado, 1–12. <https://doi.org/10.1145/2503210.2503219>
- [50] Zhang Xianyi, Wang Qian, and Zhang Yunquan. 2012. Model-driven level 3 BLAS performance optimization on Loongson 3A processor. In *2012 IEEE 18th international conference on parallel and distributed systems*. IEEE, Singapore, 684–691. <https://doi.org/10.1109/ICPADS.2012.97>
- [51] Shinhung Yang, Jiun Jeong, Bernhard Scholz, and Bernd Burgstaller. 2023. Cloudprofiler: TSC-based inter-node profiling and high-throughput data ingestion for cloud streaming workloads. [fof arXiv:2205.09325](https://arxiv.org/abs/2205.09325) [cs.DC]
- [52] Shaobin Zhan and Hongying Huo. 2012. Improved PSO-based task scheduling algorithm in cloud computing. *Journal of Information and Computational Science* 9 (11 2012), 3821–3829.
- [53] Honglin Zhang, Yaohua Wu, and Zaixing Sun. 2022. EHEFT-R: multi-objective task scheduling scheme in cloud computing. *Complex and Intelligent Systems* 8 (2022), 4475–4482. <https://doi.org/10.1007/s40747-021-00479-7>
- [54] Xiangchen Zhao, Diyi Hu, and Bhaskar Krishnamachari. 2021. Design and Experimental Evaluation of Algorithms for Optimizing the Throughput of Dispersed Computing. <https://doi.org/10.48550/ARXIV.2112.13875> arXiv:2112.13875 [cs.DC]